Geosciences and Engineering, Vol. 12, No. 1 (2024), pp. 5–19.
https://doi.org/10.33030/geosciences.2024.01.001

JOINT INVERSION OF LABORATORY-MEASURED ACOUSTIC PHASE VELOCITY AND QUALITY FACTOR DATA

BRIGITTA TURAI-VUROM[1]*, MIHÁLY DOBRÓKA[2]
[1]**Institute of Exploration Geosciences, Department of Geophysics, University of Miskolc,*
brigitta.vurom@gmail.com
[2]*Institute of Exploration Geosciences, Department of Geophysics, University of Miskolc,*
dobrokam48@gmail.com
[1]https://orcid.org/0000-0001-7483-6458
[2]https://orcid.org/0000-0003-3956-2070

Abstract: The paper presents a new rock-physical model to describe the pressure dependences of the phase velocity and quality factor (Q). Acoustic laboratory data for P-wave velocity and Q factor were measured on the sandstone sample at 40 different pressures. The spectral ratio method was used to measure the Q factor data utilizing an aluminum sample (with the size and geometry of the rock sample) as a reference. The measured velocity and Q factor data were processed in an inversion procedure. The results showed that both the velocity-pressure and the Q factor pressure dependence can be well-described utilizing the newly developed rock-physical model in forward modeling. From the estimated inversion parameters, v_p and Q can be calculated for the full pressure range.

Keywords: *model development, acoustic P wave velocity, quality factor, inversion, pressure dependence*

1. INTRODUCTION

There is a growing claim to predict rock physical parameters more accurately at various geological structures. Geophysics has a wide palette to determine these parameters, for example, acoustic velocity, porosity, permeability, and elastic moduli and it is well-known that pressure has a strong influence on them. The change of acoustic wave velocity propagating in rocks under pressure is highly nonlinear. To explain the phenomenon various models and empirical relations were developed.

It is observed that pressure has more influence on velocities in the beginning phase of loading, later it lessens and the velocities tend to have a limit value. The basic concepts link the pressure dependence of velocity and Q factor to the change in pore volume or closure of microcracks due to the increasing load, as Birch (1960) or Brace and Walsh (1964) proposed in their studies. This paper focuses on a combination of the two concepts because they simultaneously occur under real petrophysical conditions. When increasing pressure acts on rock, the microcracks are closing and at the same time grains become closer to each other (compaction occurs in the grain structure). Both the closing of the microcracks and the decrease in pore volume cause an increase in the propagation velocity and Quality factors. In the knowledge of the pressure dependence, we can estimate the pressure (pore pressures) under real condition (Dócs and Baracza, 2022; Nagy et al., 2019a; Nagy et al., 2019b). In what follows the combined petrophysical model will be presented. The model will be validated in its application in the interpretation of laboratory-measured velocity- and Q-factor data.

2. THE COMBINED ROCK-PHYSICAL MODEL

There are two basic ideas to explain the pressure dependence of the propagation characteristics of seismic waves: Brace and Walsh (1964) declared that the main factor is the closure of the microcracks, while Birch (1960) suggested a mechanism in which an increasing pressure produces a reduction in the pore space followed by the increasing contact between the grains of the rock. Following Brace and Walsh (1964) a rock-physical model was introduced by Dobróka and Somogyi-Molnár (2012) while the model based on the concept of Birch (1960) was published by Somogyi Molnár et al. (2015). In real rock conditions both two mechanisms (microcracks closure and pore volume reduction) can occur, thus in the following we present a combined petrophysical model based on the results of Dobróka and Somogyi-Molnár (2012) and Somogyi Molnár et al. (2015).

2.1. The microcracks model

The basic assumption of the proposed model is that the *dN* change in the number of microcracks is directly proportional to the applied stress increase $d\sigma$ and the *N* total number of microcracks (per unit volume) expressed by the differential equation

$$dN = -\lambda N d\sigma \tag{1}$$

where λ is a proportionality constant. In *Equation (1)* the negative sign represents that at increasing stress – with closing microcracks – the number of the open microcracks decreases. Solving *Equation (1)* we find

$$N = N_0\, exp(- \lambda\sigma) \tag{2}$$

where N_0 is the number of the open microcracks at a stress-free state $(\sigma = 0)$. The second item of building the model is the assumption of a linear relationship between the propagation velocity change *dv* – due to pressure increment $d\sigma$ – and *dN*

$$dv = -\alpha dN \tag{3}$$

where α is amaterial quality dependent constant. The negative sign represents that the velocity is increasing with decreasing number of cracks. Combining *Equation (3)* with *Equation (1)* and *(2)*, we obtain

$$dv = \alpha\lambda N_0\, exp(- \lambda\sigma) d\sigma. \tag{4}$$

Solving the upper differential equation we have

$$v = K - \alpha N_0 \, exp(-\lambda\sigma) \tag{5}$$

where K is an integration constant. At a stress-free state ($\sigma = 0$) the propagation velocity v_0 can be measured and computed from *Equation (5)* as $v_0=K-\alpha N_0$. Hence, we obtain the integration constant as $K=v_0+\alpha N_0$. After this *Equation (5)* can be rewritten as

$$v = v_0 + \Delta v(1 - exp(-\lambda\sigma)) \tag{6}$$

where the notation $\alpha N_0 = \Delta v$ has been used. *Equation (6)* provides a theoretical connection between the propagation velocity and rock pressure. The model equation shows that the propagation velocity – as a function of stress – starts from v_0 and increases up to the $v_{max}=v_0+\Delta v$ value according to the function of $1\text{-}exp(-\lambda\sigma)$. Thus, the value $\Delta v = v_{max} - v_0$ specifies a velocity range in which the propagation velocity can vary from the stress-free state up to the state characterized by high rock pressure. Constant λ is called the stress sensitivity.

2.2. The pore volume model

In accepting the idea of Birch (1960), the rock physical model explaining the physical relationship between the applied stress and the acoustic P-wave velocities is summarized here following Somogyi Molnár et al. (2015). Utilizing similar considerations as above, the basic model law can be formulated by *Equation (7)*

$$dV = -\gamma V d\sigma \tag{7}$$

where dV is the change of specific pore volume, $d\sigma$ is the applied stress increase and γ is the proportionality factor, a new rock physical parameter. The negative sign indicates that the pore volume is decreasing at increasing pressure. The solution to *Equation (7)* is

$$V = V_0 \, exp(-\gamma\sigma) \tag{8}$$

We assume also a linear relationship between the infinitesimal change of the appropriate propagation wave velocity dv and dV

$$dv = -\beta dV \tag{9}$$

where the β proportionality factor is a new material characteristic. The negative sign represents that the velocity and pore volume are inversely proportional. Combining *Equations (7)* and *(8)* and solving the differential equations as well as applying the notation $\Delta v_0=\beta V_0$ one can obtain

$$v = v_0 + \Delta v_0(1 - exp(-\gamma\sigma)) \tag{10}$$

where v_0 is the propagation velocity at a stress-free state, while the quantity Δv_0 means the velocity change caused by the presence of pores at a stress-free state (Ji et al., 2007) and can be considered as the difference between the velocities measured at maximum and zero stresses, i.e., $\Delta v_0 = v_{max} - v_0$.

The physical meaning of parameter γ was derived by Dobróka and Somogyi-Molnár (2012). It can be formulated as the logarithmic stress sensitivity of the velocity-change

$$S(\sigma) = -\frac{1}{\Delta v}\frac{d\Delta v}{d\sigma} = -\frac{d\,ln(\Delta v)}{d\sigma} = \gamma \tag{11}$$

2.3. The combined velocity model

If the two mechanisms are present, the infinitezimal velocity change should contain both sources of the stress-induced variation as

$$dv = -\alpha dN - \beta dV \tag{12}$$

or differentiating *Equations (2)* and *(8)*

$$dv = \alpha\lambda N_0 exp(-\lambda\sigma)d\sigma + \beta\gamma V_0\, exp(-\gamma\sigma)d\sigma \tag{13}$$

After integration, we can find

$$v = -\alpha N_0 exp(-\lambda\sigma) - \beta V_0\, exp(-\gamma\sigma) + C \tag{14}$$

where C is an integration constant determined using the initial condition that at stress-free state $(\sigma = 0)$ the propagation velocity is v_0

$$v_0 = -\alpha N_0 - \beta V_0 + C \tag{15}$$

resulting in

$$C = v_0 + \alpha N_0 + \beta V_0 \tag{16}$$

and also

$$v = v_0 + \alpha N_0(1 - exp(-\lambda\sigma)) + \beta V_0(1 - exp(-\gamma\sigma)) \tag{17}$$

This is the derived formula for the combined rock physical model.

The experiences show, that in most cases closing pores requires much higher pressure compared to the closing of microcracks, or in other words, the characteristic pressure $1/\gamma$ of the mechanism of closing the pores is much higher compared to $1/\lambda$ (the characteristic pressure belonging to the mechanism of closing microcracks). This means that in *Equation (17)*

$$\gamma\sigma \leq\leq \lambda\sigma \tag{18}$$

In such cases, *Equation (17)* can be simplified, because at moderate pressures the second exponential function can be replaced by its truncated Taylor series as

$$exp(-\gamma\sigma) \cong 1 - \gamma\sigma \tag{19}$$

Inserting this into *Equation (17)* we find

$$v = v_0 + \alpha N_0(1 - exp(-\lambda\sigma)) + \beta V_0 \gamma\sigma \tag{20}$$

or introducing the notations $\alpha N_0 = \Delta v$ and $D = \beta V_0 \gamma$ we find a simplified model equation

$$v = v_0 + \Delta v(1 - exp(-\lambda\sigma)) + D\sigma \tag{21}$$

This relationship is extensively used in rock physics as an empirical equation, e.g., in Ji et al. (2007), Wepfer and Christensen (1991), Wang et al. (2005), Stierman et al. (1979), Yu et al. (1993), etc. The above considerations can serve as theoretical background behind a previously introduced empirical formula.

2.4. The combined Q-factor model

We assume that the pressure dependence of the Q factor is influenced by the same intrinsic mechanisms (closing of microcracks and change in the pore volume) as it was assumed in the case of phase velocity. Consequently, the infinitezimal change in the Q factor should contain both sources of the stress-induced variation as

$$dQ = -\eta dN - \kappa dV \tag{22}$$

where the proportionality factors η and κ are new material characteristics. After differentiating *Equations (2)* and *(8)* we find

$$dQ = \eta\lambda N_0 exp(-\lambda\sigma)d\sigma + \kappa\gamma V_0\, exp(-\gamma\sigma)d\sigma \tag{23}$$

Repeating the above derivations, the final result is

$$Q = Q_0 + \eta N_0(1 - exp(-\lambda\sigma)) + \kappa V_0(1 - exp(-\gamma\sigma)) \tag{24}$$

where Q_0 is the Q factor at zero pressure. This is the combined Q factor formula. If the inequality (18) fulfills, *Equation (24)* simplifies as

$$Q = Q_0 + \Delta Q(1 - exp(-\lambda\sigma)) + E\sigma \tag{25}$$

where the notations $\Delta Q = \eta N_0$ and $E = \kappa V_0 \gamma$ were used. In the case of $\eta N_0 \leq\leq \kappa V_0$, *Equation (25)* gives the model assuming one mechanism

$$Q = Q_0 + \Delta Q(1 - exp(-\lambda\sigma)) \tag{26}$$

3. MEASUREMENTS AND INVERSION

To confirm the reliability of the combined model velocity, Q factor datasets were measured. The pulse transmission technique was used for wave velocity measurements and the method developed by Toksöz et al. (1979) was implemented to determine Q factor (see Appendix). We performed measurements on a fine-grained sandstone sample which was subjected to uniaxial stresses by the automatic acoustic test system of the Department of Geophysics, University of Miskolc *(Figure 1)*.

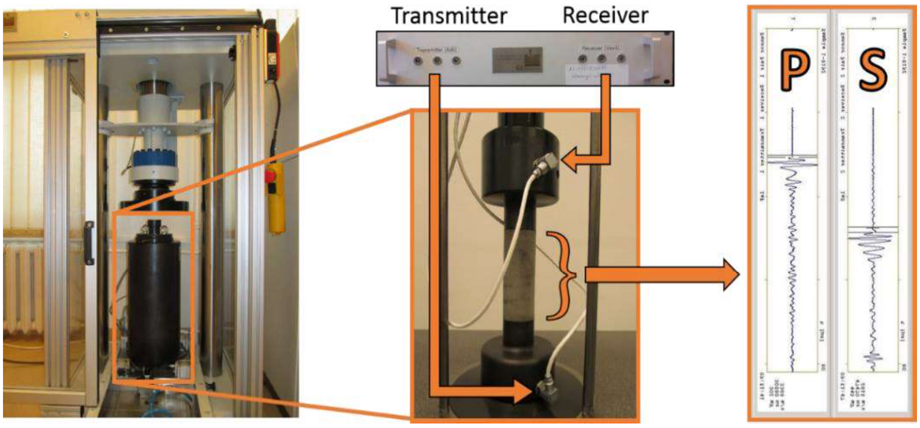

Figure 1
Experimental setup. Left: load frame and pressure cell. Middle: ultrasonic device, sandstone sample between transmitter and receiver built in the pressure stamps. Right: P and S wave arrivals

The digitally controlled test system includes a pressure cell, an ultrasonic 2-channel testing device and a load frame. P-wave velocity and Q factor – as a function of pressure – were measured at 40 discrete pressures equidistantly distributed in the [0.26, 82.15] (MPa) range. According to the Toksöz method (1979), the full waveform was also measured on the reference aluminum sample at all 40 discrete pressures. We determined the P-wave derived Q factor (Q) of the sandstone sample by calculating spectral ratios from the spectra obtained after Discrete Fourier Transformation (DFT) of the measured waveforms. (The details are presented in the Appendix.) The measured data are shown in *Figure 2*. The velocity dataset shows a linear trend at higher pressures [following *Equation (21)* while the Q factor approaches to a constant value written in *Equation (26)*] or to a slightly increasing one *[Equation (26)]*.

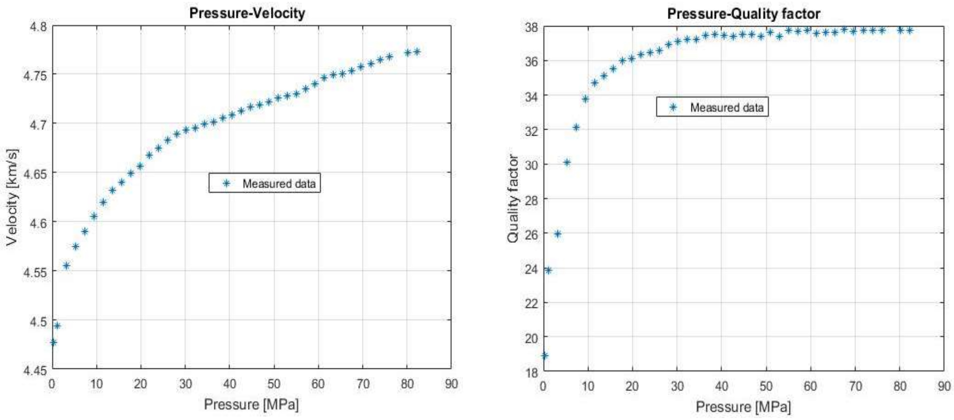

(a) (b)

Figure 2
The measurement data: a.) P-wave velocity, b.) P-wave Q factor

To prove the validity and applicability of the models introduced above, we use the measured datasets in an inversion procedure. The parameters appearing in the model equations will be determined by processing measurement data in both independent and joint inversion procedure (using the Damped Least Squares Method). In forward modeling it is obvious to choose the simplified combined model in the case of the velocity data. Because of the moderate increase of the Q factor at high pressures both the simplified combined and the one-mechanism model can be applied. For joint inversion purposes, it is useful to modify slightly the forward problem formulae and write *Equation (21)* in the form

$$v = A - Bexp(-\lambda\sigma)) + D\sigma \tag{27}$$

where $A = v_0 + \Delta v$, $B = \Delta v$. Similarly, *Equation (25)* is written in the form

$$Q = A - Bexp(-\lambda\sigma)) + E\sigma \tag{28}$$

where $A = Q_0 + \Delta Q$, $B = \Delta Q$. In the case of the one-mechanism model, *Equation (26)* is written as

$$Q = A - Bexp(-\lambda\sigma)) \tag{29}$$

For measuring the accuracy of inversion estimation, the relative estimation error is used (Menke, 1984; Gyulai et al., 2013). To characterize the fit between the measured and calculated data the relative data distance

$$d = \sqrt{\frac{1}{N}\sum_{k=1}^{N}\left(\frac{d_k^{(\mathrm{meas})} - d_k^{(\mathrm{calc})}}{d_k^{(\mathrm{calc})}}\right)^2} \cdot 100\ [\%] \tag{30}$$

is utilized. The result of the independent LSQ inversion of the P-wave velocity data is shown in *Figure 3*.

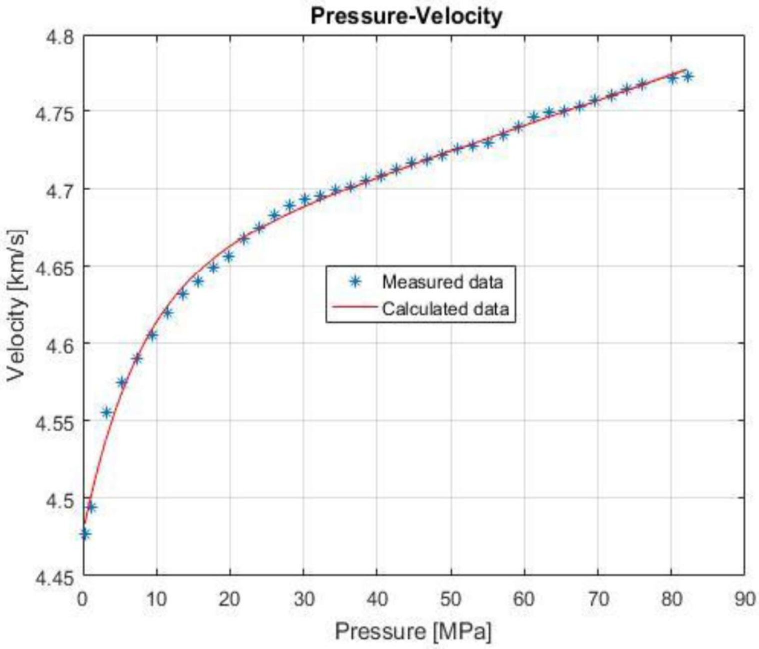

Figure 3
Inversion of P-wave velocity data using the simplified combined model [Equation (27)] in forward modeling

The estimated model parameters and the relative data distance are given in the first column of *Table 1*. In the inversion of Q factor data, we investigated two cases in selecting forward modeling. The results of the LSQ inversion with *Equation (28)* as a forward modeling formula are shown in *Figure 4*. The estimated model parameters are in the second column of *Table 1*. We can see that the value of the data distance is much larger for the Q factor than for the velocity, the reason is that the measured Q factor data are much less accurate than the velocity data, i.e., the *Q* dataset is much noisier than the *v* dataset.

Table 1

Model parameters estimated by independent LSQ inversion

Velocity inversion	Quality factor inversion I. using the combined model	Quality factor inversion II. using the one mechanism model
A = 4.642 +/– 0.071%	A = 36.582 +/– 0.609%	A = 37.473 +/– 0.231%
B = 0.165 +/– 2.447%	B = 17.382 +/– 2.038%	B = 17.941 +/– 2.030%
lambda = 0.129 +/– 5.72%	lambda = 0.181 +/– 4.74%	lambda = 0.158 +/– 3.99%
D = 0.0016 +/– 3.452%	E = 0.0168 +/– 24.33%	
d = 0.094%	d = 1.604%	d = 1.797%

In the other case, when *Equation (28)* serves as a forward modeling formula the results shown in *Figure 5* can be found. The estimated model parameters are in the third column of *Table 1*. As can be seen, the fit between the measured data is better in *Figure 4*.

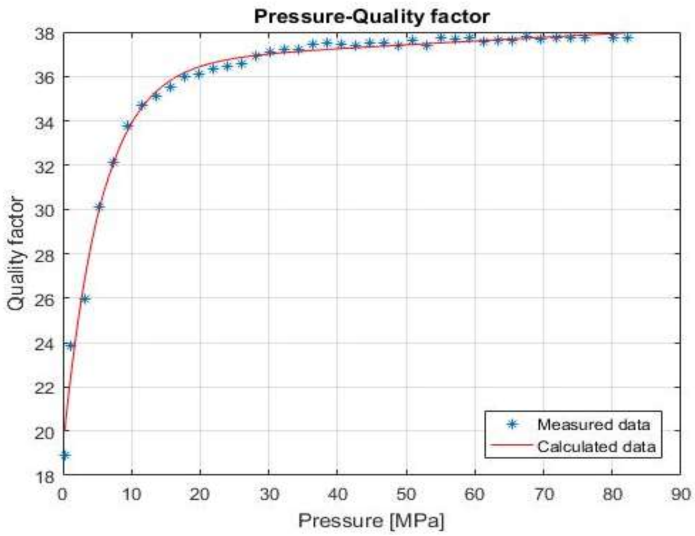

Figure 4

Inversion of P-wave Q factor data using the simplified combined model [Equation (28)] in forward modeling

The above results of independent inversion gave three different values for the lambda parameter. On the other hand, all three rock physical models in the above inversion tests were based on *Equation (1)*, which implies the same value for the lambda parameter. Because of this reason, we integrate the velocity- and Q factor datasets in a joint inversion procedure in which the connection of the two physically different kinds of measurement data set is based on the common lambda parameter.

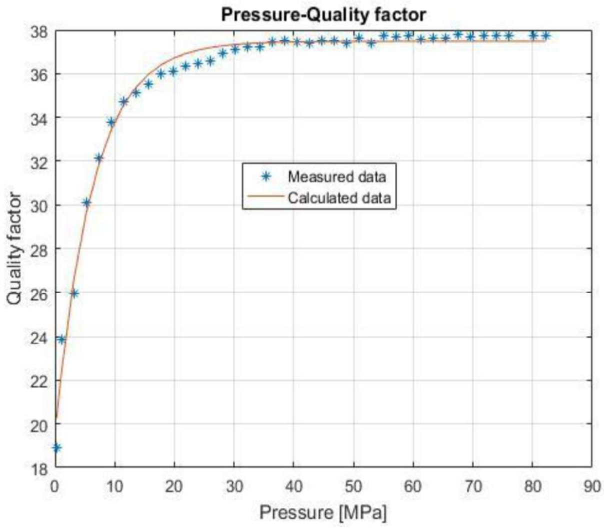

Figure 5

Inversion of P-wave Q factor data using the one mechanism model [Equation (29)] in forward modeling

In the joint inversion procedure, *Equation (27)* and *(28)* were selected as forward modeling formulae. The results are shown in *Figures 6* and *7*, the estimated parameters are given in *Table 2*.

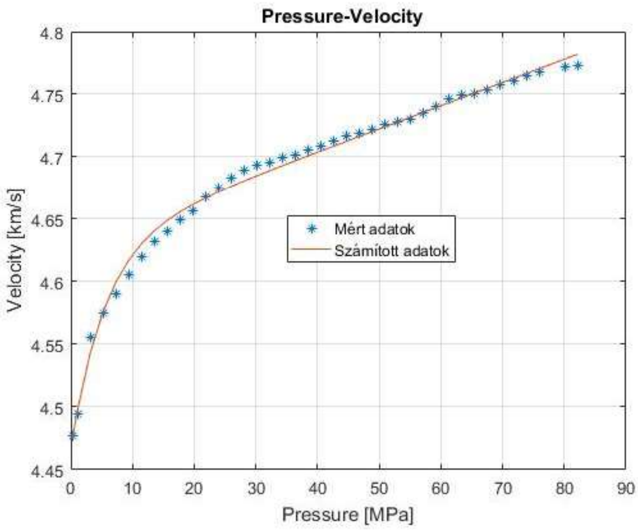

Figure 6

P-wave velocity as a function of pressure estimated by joint inversion using the simplified combined models [Equations (27) and (28)] in forward modeling

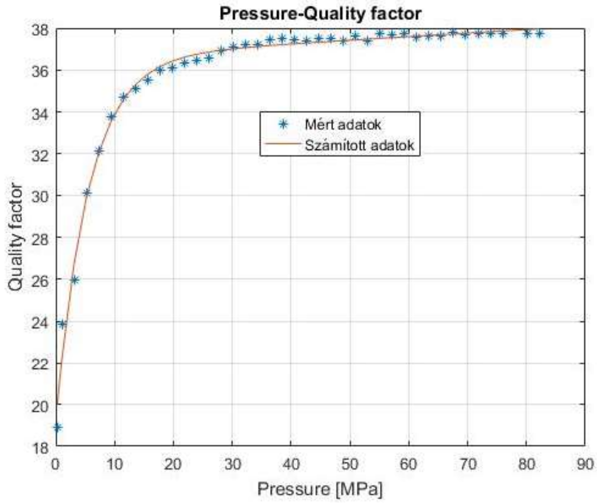

Figure 7

P-wave Q factor as a function of pressure found in joint inversion, using the simplified combined models [Equations (27) and (28)] in forward modeling

Table 2

Model parameters estimated by LSQ joint inversion

velocity parameters	Q factor parameters	Common parameter
Av = 4.629	Aq = 36.582	lambda = 0.180
Bv = 0.163	Bq = 17.382	
Dv = 0.0019	Eq = 0.0168	data distance: d = 1.137%

With the above model parameters, the pressure-dependent acoustic P-wave velocity and Q factor can be calculated for the whole pressure range by *Equations (27)* and *(28)*. The distance between the measured and calculated data is smaller, then that found in independent Q factor inversion and grater then that given by independent velocity inversion. The inversion results prove that the petrophysical model describing the pressure dependence of acoustic P-wave velocity and Q factor applies well in practice.

4. CONCLUSIONS

A fine-grained compact sandstone sample was used to measure the acoustic laboratory data of P-waves at 40 different discrete pressures in the [0.26, 82.15] (MPa) range, from which velocity-pressure and quality factor-pressure relationships were described. The spectral ratio method was used to determine the quality factor. To describe the velocity-pressure and quality factor-pressure relationships of the sandstone sample, a rock physics model is given that assumes the simultaneous presence of two mechanisms (closing of microcracks and change in the pore volume). The measured data were processed by inversion procedures and then integrated into a joint inversion procedure in order to combine the two physically different types of measurement data sets using the lambda unknown as common parameter, assuming that the pressure dependence of the quality factor is affected by the same intrinsic mechanisms as the pressure dependence of the P-wave velocity. Using the model parameters estimated by joint inversion, the pressure-dependent acoustic P-wave velocity and the quality factor can be calculated for the full pressure range, based on the forward equations. The inversion results demonstrate that the petrophysical model explaining the pressure dependence of the acoustic P-wave velocity and the quality factor is well applicable. Based on the results of the inversion calculation, it can be stated that joint inversion significantly reduces the data distance for Q factor inversions.

ACKNOWLEDGEMENTS

The research was carried out in project No. K-135323 supported by the National Research, Development and Innovation Office (NKFIH).

APPENDIX

For the laboratory determination of the quality factor (Q), Toksöz et al. (1979) developed the method of spectral ratios, which was used to evaluate our acoustic P-wave measurements. During the method of spectral ratios, we also perform a reference measurement on an aluminum sample with the same geometry as the rock sample, since the Q factor of aluminum is very high, and we can use this property well in our calculations. The amplitude spectra of the acoustic waves that can be measured on the samples can be written with the following relations

$$\boldsymbol{A_{alu}(f) = G_{alu}(x)e^{-\alpha_{alu}(f)x}e^{j(2\pi ft - k_{alu}x)}} \tag{31}$$

$$\boldsymbol{A_{rock}(f) = G_{rock}(x)e^{-\alpha_{rock}(f)x}e^{j(2\pi ft - k_{rock}x)}} \tag{32}$$

where $A_{alu}(f)$ – amplitude spectrum of the aluminum sample,
$A_{rock}(f)$ – amplitude spectrum of the sandstone sample,
$G_{alu}(x)$ – geometric factor of the aluminum sample,
$G_{rock}(x)$ – geometric factor of the sandstone sample,
x – length of the sample,
$\alpha_{alu}(f)$ – frequency-dependent attenuation factor of the aluminum sample,
$\alpha_{rock}(f)$ – frequency-dependent attenuation factor of the sandstone sample,
k_{alu} – wavenumber of the aluminum sample,
k_{rock} – wavenumber of the sandstone sample.

McDonal et al. (1958), Jackson and Anderson (1970) previously showed that in the frequency range 0.1–1 MHz the attenuation factor $\boldsymbol{\alpha}$ is a linear function of frequency which can be written as follows

$$\boldsymbol{\alpha(f) = \gamma f} \tag{33}$$

where γ is a proportionality factor. If the geometry of the aluminum sample and the rock sample are the same, the spectral ratio will be as follows

$$\frac{A_{alu}(f)}{A_{rock}(f)} = e^{-(\gamma_{alu}-\gamma_{rock})fx} \tag{34}$$

Compared to rocks, aluminum is an almost attenuation-free medium ($\gamma_{alu} \approx 0$), therefore

$$\frac{A_{alu}(f)}{A_{rock}(f)} = e^{\gamma_{rock} f x} \tag{35}$$

Thus, by taking the natural logarithm of Equation (35), we can obtain the proportionality factor γ_{rock} of the rock

$$\gamma_{rock} = \frac{ln\left(\frac{A_{alu}(f)}{A_{rock}(f)}\right)}{x\,f} \tag{36}$$

Knowing the γ_{rock} quantity, the Q factor can be determined (Toksöz et al., 1979)

$$Q = \frac{\pi}{v\,\gamma_{rock}} \tag{37}$$

where v is the velocity of the acoustic wave. Neglecting the phase shift and the measurement errors, the logarithm of the spectral ratio calculated as a function of frequency is scattered around the following equalization line

$$ln\left(\frac{A_{alu}(f)}{A_{rock}(f)}\right)_{str} = \beta f + \delta \tag{38}$$

where β – inclination angle of the equalization line,
δ – vertical axis section of the equalization line.
Based on relations (36) and (37), the value of the Q factor is given as

$$Q = \frac{\pi x f}{v\,ln\left(\frac{A_{alu}(f)}{A_{rock}(f)}\right)_{str}} \tag{39}$$

References

Birch, F. (1960). The velocity of compression waves in rocks to 10 kilobars. Part 1. *Journal of Geophysics Research,* 65, pp. 1083–1102.

Brace, W. F. and Walsh, J. B. (1964). A fracture criterion for brittle anisotropic rock. *Journal of Geophysics Research,* 69, pp. 3449–3456. https://doi.org/10.1029/JZ069i016p03449

Dobróka, M. and Somogyi-Molnár, J. (2012). The pressure dependence of acoustic velocity and quality factor: new petrophysical models. *Acta Geodaetica et Geophysica Hungarica*, 47, pp. 149–160. https://doi.org/10.1556/AGeod.47.2012.2.4

Dócs, R. and Baracza, M. K., (2022). A new method of pressure drop modelling in sandstone rocks. *Multidisciplinary Studies*, 12, 3, pp. 264–273.

Gyulai, Á., Baracza, M. K. and Tolnai, É. E. (2013): The application of joint inversion in geophysical exploration. *International Journal of Geoscience*, 4, pp. 283–299

Jackson, D. D. and Anderson, D. L. (1970). Physical mechanisms of seismic wave attenuation. *Rev. Geophys. Space Phys*., 8, pp. 1–63.

Ji, S., Wang, Q., Marcotte, D., Salisbury, M.H. and Xu, Z. (2007). P wave velocities, anisotropy and hysteresis in ultrahigh-pressure metamorphic rocks as a function of confining pressure. *Journal of Geophysics Research*, 112, B09204. https://doi.org/10.1029/2006JB004867

McDonal, F. J., Angona, F. A., Mills, R. L., Sengbush, R. L., Van Nostrand, R. G. and White, J. E. (1958). Attenuation of shear and compressional waves in Pierre shale. *Geophysics*, 23, pp. 421–439.

Menke, W. (1984), *Geophysical Data Analysis – Discrete Inverse Theory*, London, Academic Press.

Nagy, Zs., Baracza, M. K. and Szabó, N. P., (2019a). Integrated Pore Pressure Prediction with 3D Basin Modeling. *Second EAGE Workshop on Pore Pressure Prediction*, pp. 1–5., 19–21 May 2019, Amsterdam, Netherlands.

Nagy, Zs., Baracza, M. K. and Szabó, N. P., (2019b). Pore Pressure Prediction In: Pannonian Hydrocarbon Reservoir Systems Using An Integrated Interpretation Approach. *Geosciences and Engineering*, 7, 12, pp. 105–115.

Somogyi Molnár, J., Kiss, A. and Dobróka, M. (2015). Petrophysical models to describe the pressure dependence of acoustic wave propagation characteristics. *Acta Geodaetica et Geophysica*, https://doi.org/10.1007/s40328-014-0074-4.

Stierman, D. J., Healy, J. H. and Kovach, R. L. (1979), Pressure-induced velocity gradient: An alternative to a Pg refractor in the Gabilan Range, central California, *Bulletin of the Seismological Society of America*, 69, pp. 397–415. https://doi.org/10.1785/BSSA0690020397

Toksöz, M. N., Johnston, D. H. and Timur, A. (1979). Attenuation of seismic waves in dry and saturated rocks. *Geophysics*, 44 (4), pp. 681–690.

Wang, Q., Ji, S.C., Salisbury, M.H., Pan, M.B., Xia, B. and Xu, Z.Q. (2005). Pressure dependence and anisotropy of Pwave velocities in ultrahigh-pressure metamorphic rocks from the Dabie-Sulu orogenic belt (China): Implications for seismic properties of subducted slabs and origin of mantle reflections. *Tectonophys*, 398, pp. 67–99. https://doi.org/10.1016/j.tecto.2004.12.001

Wepfer, W.W. and Christensen, N.I. (1991). A seismic velocity-confining pressure relation, with applications. *International Journal of Rock Mechanics and Mining Sciences & Geomechanics,* 28, pp. 451–456. https://doi.org/10.1016/0148-9062(91)90083-X

Yu, G., Vozoff, K., and Durney, D. W. (1993). The influence of confining pressure and water saturation on dynamic elastic properties of some Permian coals. *Geophysics*, 58 (1), pp. 30–38.